JOURNALS OF CATALYSIS **159,** 140–149 (1996)
ARTICLE NO. 0073

Comparison of Partial Oxidation and Steam-CO_2 Mixed Reforming of CH_4 to Syngas on MgO-Supported Metals

Daiyi Qin,[1] Jack Lapszewicz, and Xuanzhen Jiang

Division of Coal and Energy Technology, CSIRO, Private Mail Bag 7, Menai 2234, NSW, Australia

Received April 6, 1994; revised November 25, 1994; accepted October 13, 1995

Partial oxidation (POX) and steam-CO_2 mixed reforming of CH_4 on MgO-supported noble metals were investigated at high space velocity (5.5×10^5 h^{-1}). Temperature-programmed reaction (TPR) and isotope transient techniques were used to study the mechanism of POX and mixed reforming. TPR profiles of POX and mixed reforming showed similar ignition reaction behaviors, which implied that there are similar characteristics in their mechanisms. Steam reforming and CO_2 reforming were found to start at the same time in mixed reforming. TPR and CH_4–D_2 exchange experiments indicated that CH_4 was activated at low temperature on Rh/MgO. POX showed much higher activity than mixed reforming although their C, H, and O atomic concentrations were the same at the beginning of each reaction. It is suggested that the lower rate of reaction in mixed reforming is due to the blocking of active sites for CH_4 activation by CO_2 and H_2O. It seems that the coexistence of CO_2 and H_2O shows stronger inhibition than that of CO_2 alone and H_2O alone. Rh/MgO without previous reduction treatment also showed a high reactivity for POX but with a higher ignition temperature than a prereduced catalyst. With regard to the H_2/CO ratio, mixed reforming showed a changing ratio with increasing temperature, which suggested that the rate for CO_2 reforming increases faster than that of steam reforming. An *in situ* isotope-labelled $^{13}CO_2$ transient experiment for mixed reforming indicated that carbon formed from CO_2 or CO decomposition was less active than $(CH_x)_{ad}$ ($x = 0$, 1, 2, and 3) formed from CH_4 decomposition. For POX, a small amount of steam had little effect on CO formation rate for an active catalyst, e.g., Rh/MgO or Ru/MgO, but decreased the rate for less active catalyst Pt/MgO. All the results indicated that steam reforming and CO_2 reforming in mixed reforming start simultaneously and have the same type of reaction intermediate, adsorbed atomic oxygen. POX proceeds via both one-step and two-step mechanisms, the ratio for each mechanism being dependent on the concentration and kinetics of adsorbed atomic oxygen and gaseous atomic oxygen. Mechanisms for POX and mixed reforming are suggested and the effect of oxygen–metal bond strength on activity is discussed.

INTRODUCTION

To convert natural gas into high-value products has been a focus of research for many years. Syngas plays a key role as a feedstock in many synthesis processes in modern chemical industry. Conventionally, syngas is produced by steam reforming of natural gas (1). Recently, partial oxidation (POX) (2–7) and CO_2 reforming (8, 9) of natural gas to syngas have attracted much academic and industrial interest because of their potential to reduce the cost of syngas or for application in energy storage technology. The overall stoichiometries for the three reactions are:

$$CH_4 + H_2O \rightarrow CO + 3H_2 \quad (-\Delta H^\circ_{298} = -206 \text{ kJ/mol}) \quad [1]$$

$$CH_4 + 1/2\,O_2 \rightarrow CO + 2H_2 \quad (-\Delta H^\circ_{298} = 38 \text{ kJ/mol}) \quad [2]$$

$$CH_4 + CO_2 \rightarrow 2CO + 2H_2 \quad (-\Delta H^\circ_{298} = -247 \text{ kJ/mol}). \quad [3]$$

Steam reforming (reaction [1]) has been extensively studied, particularly on Ni catalysts (1), and it has two distinct drawbacks. The reaction is strongly endothermic and there is a larger H_2/CO ratio than is required for subsequent processes. POX (reaction [2]) produces syngas in a mildly exothermic reaction and there is a smaller H_2/CO ratio.

POX was suggested to proceed via a two-step mechanism in which there is first deep oxidation of a part of the CH_4 to CO_2 and steam, then reforming of the remaining CH_4 with CO_2 and steam to syngas (2–4). However, a direct partial oxidation mechanism (one-step mechanism) was also suggested when some very high activities for POX were observed under high-space velocity conditions (6, 7). The reaction scheme for both routes is shown in Fig. 1.

The second step of the two-step mechanism is a combination of steam reforming (reaction [1]) and CO_2 reforming (reaction [3]) and is hereafter called mixed reforming (reaction [4]).

$$CH_4 + 2/3\,H_2O + 1/3\,CO_2 \rightarrow 4/3\,CO + 8/3\,H_2 \quad (-\Delta H^\circ_{298} = -219 \text{ kJ/mol}). \quad [4]$$

[1] To whom correspondence should be addressed. Present address: Department of Chemical Engineering, University of Bradford, Bradford, West Yorkshire, BD7 1DP, United Kingdom.

0021-9517/96 $18.00

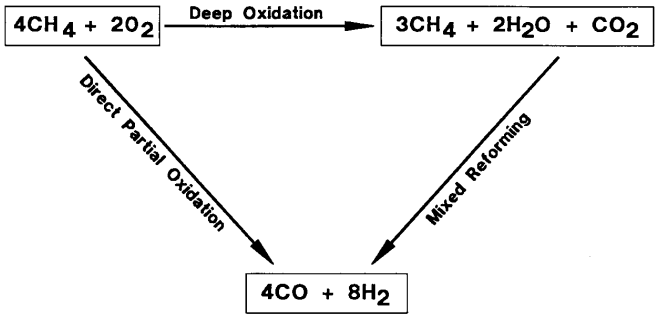

FIG. 1. Suggested reaction scheme for POX.

To check the mechanism of POX, it is useful to compare the reactivities of mixed reforming with POX using the molecular ratios indicated in Fig. 1. In this way, the atomic concentrations of C, H, and O in the reactor for both reactions are the same. If the reactivities were identical, POX might proceed via mixed reforming to produce syngas (two-step mechanism). This was the initiative for the work being carried out. Furthermore, as shown in Eq. [4], mixed reforming can adjust the H_2/CO ratio of steam reforming alone and make good use of CO_2, a major by-product of syngas production. CO_2 reforming itself exists extensively in conventional steam reforming processes because steam and CO_2 are connected through the water–gas shift reaction (WGS),

$$CO + H_2O \rightleftharpoons CO_2 + H_2 \quad (-\Delta H^\circ_{298} = 41 \text{ kJ/mol}). \quad [5]$$

While the mechanism for steam reforming on Ni catalyst has been extensively investigated (1), there has been little discussion of CO_2 reforming and even less on mixed reforming.

CO_2 reforming (reaction [3]) alone has been practised in industry (10–14) and studied for CO_2-consuming and chemical energy transmission technology (8, 9) in recent years. Although some attention has been paid to CO_2 reforming, relatively few papers have dealt with its catalytic mechanism (1). Bodrov and Apel'baum (10) suggested that CO_2 is shifted to CO and H_2O through reverse WGS, then H_2O is reacted with CH_4 (steam reforming) to produce syngas. Bodrov and Apel'baum also reported a study of the reaction kinetics, which indicated that the kinetic data for CO_2 reforming could be represented by a kinetic expression obtained for steam reforming under similar conditions on a Ni film. A similar result was reported by Rostrup-Nielsen *et al.* (15). Erdöhelyi *et al.* (16) and Rostrup-Nielsen and Bak Hansen (8) suggested a mechanism involving the dissociation of CO_2 and H_2 acceleration.

In this paper, we report and compare the results of isotope exchange, temperature-programmed reaction (TPR), and reactivities of POX and mixed reforming, suggest the mechanisms for POX and mixed reforming, and discuss the function of the oxygen–metal bond strength in the reaction kinetics for the two reactions. The effect of a small amount of steam on the activity for POX is also investigated.

EXPERIMENTAL

A fixed bed quartz microreactor (4 mm i.d.) was used in all experiments. Flows of gases (CH_4, H_2, CO_2, He, and N_2) into the reactor were controlled by mass flow meters (Brooks 5850 TR) and a controller (Brooks 5878). The steam was fed into the reactor by bubbling a carrier gas. The reaction temperatures were monitored by a sheathed thermocouple (0.4 mm o.d.) located in the middle of the catalyst bed and by a temperature programmer/controller (RKC PS-962). The exit gas analysis system consisted of two gas chromatographs (Shimadzu 8A instrument with a TCD detector and a HP-3392A integrator, Carbosphere 80/100 from Alltech Co. column 3.2 mm o.d., 3.0 m long in program temperature mode for analysis of CO, CO_2, and hydrocarbons, and Chromosorb 102 from Alltech Co. for analysis of H_2) and a quadrupole mass spectrometer (VG SX 200, enclosed source, triple filter and SEM detector) controlled by an IBM XT. Water in the exit gas was condensed by the ice/dry-ice trap before the gas chromatographs and the quadrupole mass spectrometer. All catalysts used in this study were prepared by the incipient wetness technique using aqueous solution of an appropriate metal chlorides. The amount of metal was 0.5% weight of total catalyst. Univar grade MgO from Ajax Chemicals (117 m^2/g, BET method, size <100 μm) was used as a support for all catalysts. Prior to each experiment the catalyst sample (10 mg) was reduced in a flow of H_2 (50 ml/min) at 500°C for 10 h.

Evaluation of catalytic activity for POX and mixed reforming was carried out as follows. A mixture of gases and steam with $CH_4:H_2O:CO_2:N_2 = 2.7:1.8:0.9:7.2$ mmol/s/g for mixed reforming and $CH_4:O_2:N_2 = 3.6:1.8:7.2$ mmol/s/g for POX, N_2 as a diluent and carrier gas, was passed through the catalyst bed at space velocity of 5.5×10^5 h^{-1} (contact time 6.5 ms). The activity was measured over the range 600 to 900°C. The effect of a small amount of steam on POX activity was carried out by adding steam into the POX reactor but keeping the space velocity constant. The amount of steam added was that required to give thermal balance for combined POX and steam reforming, namely, $CH_4:H_2O:O_2:N_2 = 3.8:0.6:1.6:6.6$ mmol/s/g, and was controlled by controlling the temperature of the water evaporator and, in turn, the saturated pressure of steam and its partial pressure in the feed stream. The calculation of thermodynamic equilibrium was carried out using a software and database developed by CSIRO, Australia, which considered all thermodynamic possibilities and gave the optimising composition of final reaction mixture in thermodynamic equilibrium from the input compositions of reactants.

Isotope transient experiments were carried out on the active Rh/MgO catalyst in two ways. CH_4–D_2 exchange experiments were described elsewhere (17) and a ^{13}C isotope-labelled $^{13}CO_2$ experiment in mixed reforming was carried out as follows. A mixture of CH_4, CO_2, H_2O, and He was passed over Rh/MgO at 700°C with all other conditions set the same as those in normal mixed reforming except for using He instead of N_2 as a carrier gas. After the reaction was stable, $^{13}CO_2$ (ratio-of-^{13}C-to-total carbon >99%, supplied by Cambridge Isotope Laboratories, USA) was switched into the mixture using a six-way valve to replace the CO_2 stream. The amount of $^{13}CO_2$ was enough to replace all CO_2 in the reactor and be analysed without any effect from the unlabelled CO_2 stream. The sample collecting time was precalculated in order to catch the desired products. The analytical method was a combined GC and MS method, similar to that of the CH_4–D_2 exchange experiments.

TPR experiments for POX and mixed reforming were carried out over Rh/MgO from 100 to 900°C with same reactant components and space velocity as those of POX and mixed reforming, respectively, except for using He instead of N_2 as a carrier gas at atmosphere pressure. The reactor temperature was increased at a rate of 20°C/min. The effluent from the reactor was passed though an ice/dry-ice trap and then into the sample chamber of the MS. The MS was operated in a multichannel mode to analyse CH_4, O_2, CO, and CO_2 simultaneously.

RESULTS

1. CH_4–D_2 Exchange Experiments on Rh/MgO

CH_4–D_2 exchange experiments were carried out on Rh/MgO under space velocity the same as that in POX or mixed reforming. The results are shown in Fig. 2. CH_2D_2 can be positively detected by the employed analytical techniques but can not be found in products. The exchange reaction happens from about 300°C and accelerates following the increase of temperature. At 500°C, CH_4 conversion is over 90% and CD_4 selectivity is about 70%. The result indicates that CH_4 activation is very effective on Rh/MgO.

2. Temperature Programmed Reaction (TPR)

The TPR profiles ("spectra") of POX and mixed reforming between 500 to 640°C are shown in Figs. 3 and 4, respectively. In Figs. 3 and 4 the ion current signals which are proportional to concentration are given for mass-to-charge-ratio (m/z) 15 (CH_4), 28 (CO), and 44 (CO_2). Mass 32 (O_2) is also given in Fig. 3 but H_2 and H_2O were not analysed.

In Fig. 3 at 550°C, there are sharp changes of all signals which indicate that the partial oxidation of CH_4 ignites at this point. The increase of CO and CO_2 signals and the decrease of CH_4 and O_2 signals imply that CH_4 and O_2 react with each other and produce CO and CO_2. The figure shows that the decrement of CH_4 roughly equals the sum

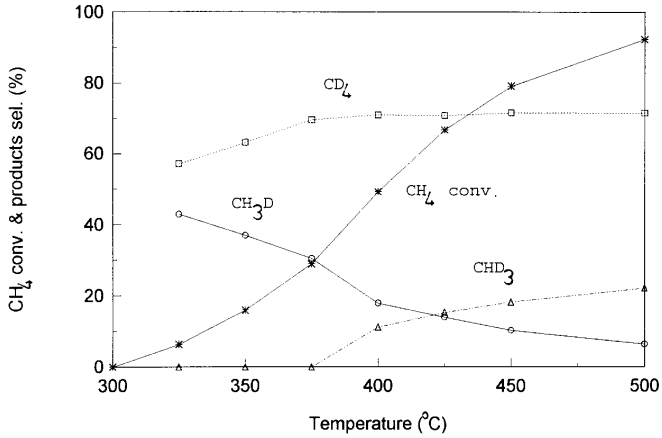

FIG. 2. Results of CH_4–D_2 exchange experiment on Rh/MgO.

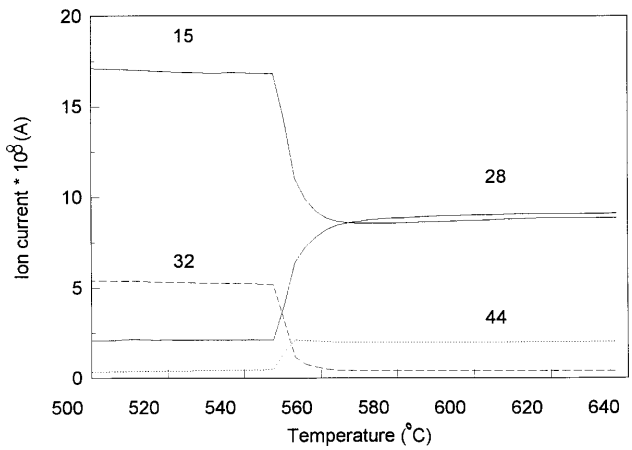

FIG. 3. TPR spectra of POX on Rh/MgO. m/z 15 = CH_4, 32 = O_2, 28 = CO, 44 = CO_2.

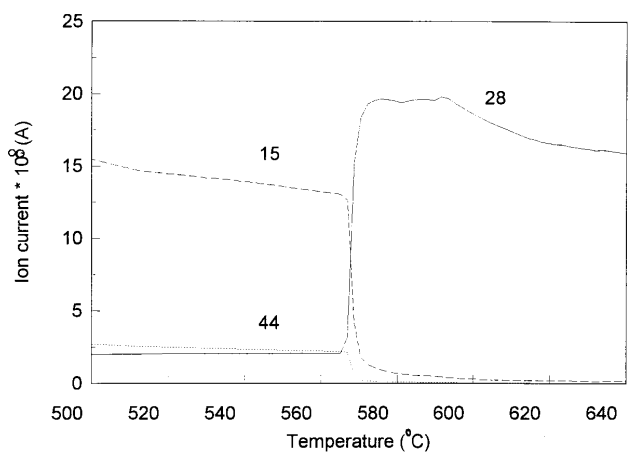

FIG. 4. TPR spectra of mixed reforming on Rh/MgO. m/z 15 = CH_4, 28 = CO, 44 = CO_2.

of increments of CO and CO_2 with CO higher than CO_2 at 550°C.

Similar sharp changes of all signals were observed for mixed reforming of CH_4 in Fig. 4. The sharp changes of all signals indicate that the mixed reforming of CH_4 ignites at 570°C. The decrease of CH_4 and CO_2 and increase of CO show that CH_4 and CO_2 react with each other and produce CO. Although CO_2 reacts with CH_4 in a molar ratio of one according to reaction [3], the decrement of CH_4 appears much larger than that of CO_2. The observation implies that steam reforming is also occurring and both reformings occur simultaneously.

The similar ignition reaction phenomena in TPR spectra for POX and mixed reforming are an indication that there are similar characteristics in their mechanisms. As CH_4 activation is the same for both reactions, the production of a similar reaction intermediate involving oxygen is expected. The mechanisms will be discussed later.

CH_4 signals in both figures show clear decreases before reaction starts but no other carbon species signal increases. The decrease begins from about 300°C and gradually accelerates up to the point of reaction start-up in each reaction. The decrease is in agreement with the result of CH_4–D_2 exchange experiments and indicates the adsorption and activation of CH_4 on the catalyst surface. In mixed reforming, CO yield is very high after the reaction starts but gradually decreases until about 700°C, then increases again with increasing temperature. The decrease of CO yield may be the effect of WGS, which produces CO_2 from CO. The effect of WGS is not prominent in POX because H_2O concentration is very low.

3. Activity

The reactions of POX and mixed reforming were carried out in a fixed-bed microreactor on several noble metal catalysts supported on MgO. Both reactions used the same space velocity as used in CH_4–D_2 and TPR experiments. The molecular ratio used in mixed reforming was according to the assumption that a quarter of the CH_4 in POX was consumed by deep oxidation with O_2. The molecular ratios used in POX and mixed reforming are simply shown in Fig. 1. In this way, POX and mixed reforming have the same C, O, and H atomic compositions at the beginning of both reactions.

CH_4 conversions for POX and mixed reforming and CO selectivities for POX are shown in Figs. 5–7. The thermodynamic equilibrium curve is also drawn in each figure for reference. CO is the only important carbon-containing product in mixed reforming, the selectivity to amorphous carbon being less than 5%. CO selectivity for mixed reforming is not drawn and discussed here.

POX exhibits ignition reaction phenomena on each metal catalyst as shown by TPR of Rh/MgO in the previous section. The ignition temperature depends on each catalyst;

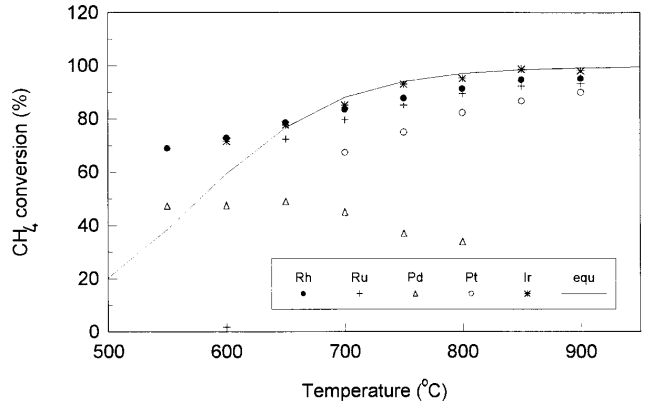

FIG. 5. CH_4 conversion of POX on MgO-supported noble metals.

it is 500°C for Pt/MgO, 550°C for Rh/MgO, and 620°C for Ru/MgO. Before the ignition, CH_4 conversion is less than 5%; however, after the ignition, CH_4 conversion becomes very high, for Rh/MgO, Ir/MgO, and Ru/MgO even higher than the calculated thermodynamic equilibrium. At the same time CO selectivity is also very high (Figs. 5 and 6). CO and CO_2 are two major carbon-containing products, and selectivity to C_2 products is less than 2%. O_2 conversion is about 96–98% for each catalyst.

Some authors (6, 7) reported high CH_4 conversion and CO selectivity for POX at very high space velocity. However, others (18, 19) have shown that CH_4 conversion and CO selectivity do not exceed the value of thermodynamic equilibrium at the reaction temperature because there can be a significant difference between the recorded temperature and the actual temperature on the catalyst surface. The temperature difference was noticed but not measured in our experiments, unfortunately.

Apart from the high CH_4 conversion and CO selectivity for POX, a very low CH_4 conversion for mixed reforming is observed for each catalyst (Fig. 7). The highest CH_4 conversion is 99%, which corresponds to the complete con-

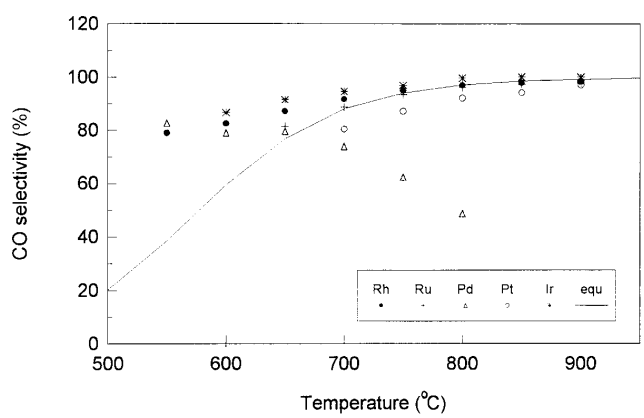

FIG. 6. CO selectivity of POX on MgO-supported noble metals.

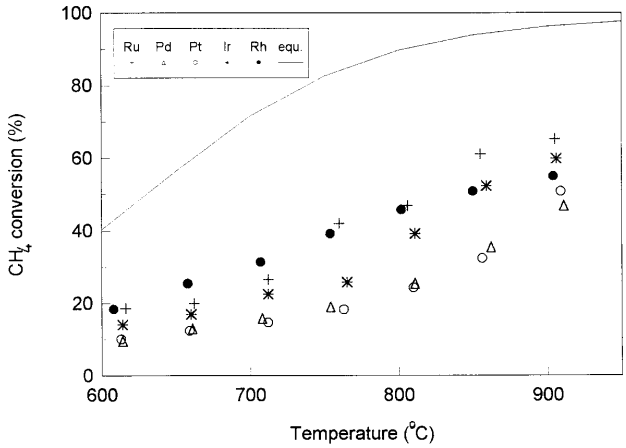

FIG. 7. CH_4 conversion of mixed reforming on MgO-supported noble metals.

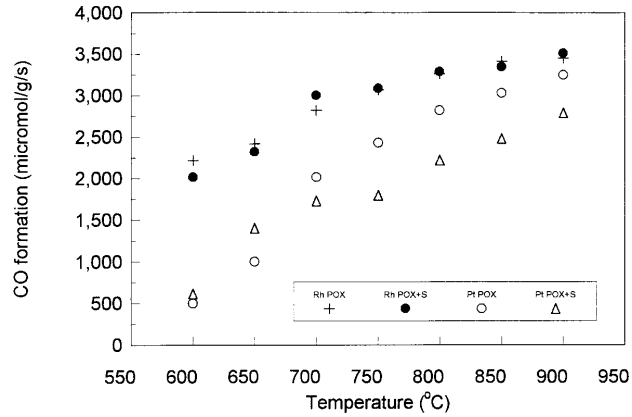

FIG. 8. Comparison of CO formation rate between POX alone and the combination of POX and steam-reforming (POX + S) on Rh/MgO and Pt/MgO.

sumption of CO_2 and steam at high temperature according to the calculation from thermodynamic data. However, the experimental data are much lower than the value of thermodynamic equilibrium at all temperatures. At 600 and 900°C, the CH_4 conversions for equilibrium are 42 and 99%, respectively; while those measured are about 15 and 50%, respectively. The activity decreases following the order Ru, Rh > Ir > Pt, Pd. The lower activity for mixed reforming may be caused by the high concentration of H_2O and CO_2 in the reactor, which blocked the active sites on the catalyst surface for CH_4 dissociation. This retarding effect of steam or CO_2 was also observed in steam reforming (20). However, it is noted that CH_4 conversion of steam reforming alone or CO_2 reforming alone on Rh/MgO or Ru/MgO reached the value of thermodynamic equilibrium at over 800°C by using the same space velocity as in POX or mixed reforming (21). It may be suggested that CO_2 and H_2O when presented together in the reactor are stronger inhibitors than CO_2 alone and H_2O alone.

Pd/MgO shows decreases of CH_4 conversion and CO selectivity for POX following the increase of temperature. The decrease probably results from coking or sintering of the catalyst. Deactivation was not observed under our experimental conditions on any catalysts, except Pd/MgO for POX, during the experiment period. No coking was found over Rh or Ru catalyst. A little amorphous carbon appeared on Pt and Pd catalysts. Rh and Ru do not readily form coke because of their low carbon diffusion rate from surface to bulk (22).

An experiment with a Rh/MgO catalyst without previous reduction treatment was also carried out. It is found that the ignition temperature was increased to 620°C but CH_4 conversion and CO selectivity were as same as those with a prereduced Rh/MgO catalyst. As oxide covers the surface of the unreduced catalyst, the results imply that the oxygen–metal bond is involved in the reaction kinetics.

4. Combination of POX and Steam Reforming

The combination of POX and steam reforming was investigated for two reasons. One reason was that if exothermic heat from POX is not removed from the reactor it would cause an undesired temperature increase and perhaps serious coking and/or sintering of the catalyst. The heat can be absorbed by the endothermic heat of steam reforming. Another reason is to investigate the effect of steam on the activity of POX.

CO formation rates of both the combination of POX and steam and POX alone are shown in Fig. 8 for Rh/MgO and Pt/MgO. The results are the same for the two reactions within the experimental error for Rh/MgO but the combination reaction shows a lower CO formation rate than POX alone for Pt/MgO. The results indicate that CH_4 conversion and CO selectivity for the combination of POX and steam reforming are similar to those of POX alone on active catalysts, such as Rh or Ru, but lower than those of POX alone on a less active catalyst, such as Pt.

5. H_2/CO Ratio

H_2/CO ratio is an important property for syngas production. Table 1 shows H_2/CO ratios of different reactions for syngas production on Rh/MgO at 600–900°C. Those of steam reforming alone and CO_2 reforming alone are also listed in Table 1 for comparison. All reactions have the same space velocity. The H_2/CO ratio of POX is close to 2.0, its stoichiometric value. The combination of POX and steam shows a stable H_2/CO ratio of about 2.25, a little larger than that of POX. This fact combined with the result from the activity experiments suggests that the existence of a small amount of steam does not change the CO formation rate but increases the H_2 formation rate compared with that of POX alone on Rh/MgO catalyst. The result also indicates that steam reforming and POX could react together on Rh/MgO.

TABLE 1

Comparison of the H_2/CO Ratio for Syngas Production Reactions on Rh/MgO at 600–900°C

Temperature (°C)	POX	Mixed reforming	POX + S[a]	Steam reforming	CO_2 reforming
600	2.0	3.9	2.3	9.3	0.8
650	1.9	2.8	2.3	5.3	1.0
700	1.8	2.3	2.1	4.3	1.0
750	2.2	2.0	2.3	3.8	1.1
800	2.2	2.0	2.2	3.6	1.1
850	2.2	1.9	2.3	3.4	1.1
900	2.1	1.7	2.3	3.3	1.1

[a] POX + S combination of partial oxidation and steam-reforming of CH_4.

Mixed reforming has H_2/CO ratios between steam reforming alone and CO_2 reforming alone, as expected. The H_2/CO ratio gradually decreased from 3.9 at 600°C to 1.7 at 900°C. As the reaction shifts from pure steam reforming to pure CO_2 reforming, the theoretical H_2/CO ratio decreases from 3 to 1. The observed decrease of H_2/CO ratio indicates an increase of the rate of CO_2 reforming relative to that of steam reforming. When considering the effect of WGS, CO_2 and H_2 were converted to CO and H_2O for a decrease of H_2/CO ratio. It appears that increase of the rate of CO_2 reforming was faster than that of steam reforming when temperature increased. The result implies that mixed CO_2 and steam reforming cannot achieve a steady H_2/CO ratio when temperature changes; the behavior is different from that of POX.

Temperature has a strong effect on H_2/CO ratio. Nevertheless, the difference among Ru, Rh, and Ir is very small, as shown in Table 2. This implies that the reaction mechanism on these noble metals for each respective syngas production method is similar.

6. In situ Isotope-Labelled $^{13}CO_2$ Transient Experiment for Mixed Reforming

^{13}C isotope-labelled $^{13}CO_2$ was used to replace the normal CO_2 in mixed reforming. The results are shown in Table 3. The relative amounts of labelled and unlabelled species are calculated from the relative peak heights of the specific species in the MS spectrum.

TABLE 2

H_2/CO Ratio on Noble Metals at 800°C

Metal	Temperature (°C)	POX	Mixed reforming	Steam reforming	CO_2 reforming
Ru	800	2.2	2.3	2.8	1.0
Rh	800	2.2	1.9	3.6	1.1
Ir	800	—	1.9	3.2	1.0
Pt	800	1.8	2.1	4.4	0.8
Pd	800	1.2	2.1	3.6	0.9

TABLE 3

Results of ^{13}C Isotope-Labelled $^{13}CO_2$ in Mixed Reforming at 700°C

Species:	CH_4	$^{13}CH_4$	CO	^{13}CO	CO_2	$^{13}CO_2$
m/z	16	17	28	29	44	45
Height	100.0	2.6	100.0	72.	79.1	100.
Ratio[a]:	$^{13}CH_4/CH_4$		$^{13}CO/CO$		$^{13}CO_2/CO_2$	
	2.5%		42%		56%	

[a] The concentration ratios of labelled and unlabelled CH_4, CO, and CO_2 are calculated from the relative height ratios of the particular species concerned.

Most of the ^{13}C is the form of ^{13}CO and $^{13}CO_2$. The amount of labelled carbon ^{13}C in the form of $^{13}CH_4$ is much less than that of ^{13}CO or $^{13}CO_2$.

DISCUSSION

1. CH_4 Dissociation and its Reactive Potential

CH_4 has a stable molecular structure. Activating CH_4 requires a high reaction temperature in most cases. However, noble metals are found to be good at activating CH_4 at reasonably low temperature. CH_4–D_2 exchange experiments on Rh film were reported by Kemball (23) and Frennet *et al.* (24). It was found that H_2 evolved on CH_4 chemisorption at about 200°C but adsorbed hydrocarbon fragments $(CH_x)_{ad}$ ($x = 0, 1, 2,$ and 3) remained on the surface at that temperature. This implied that H was easier to recombine and desorb from catalyst surface than $(CH_x)_{ad}$ ($x = 0, 1, 2,$ and 3). Under our experimental conditions, desorbed isotope exchanged products from Rh/MgO appeared from 300°C and the exchange rate increased following the increase of temperature. The type of catalyst and reaction condition, such as size of metal cluster, contact time, and partial pressure of CH_4, may affect the hydrocarbon appearance temperature. Frennet *et al.* (24) also indicated that a cluster of 7.8 Rh atoms was covered by chemisorbed CH_4, which implied that the ability of dissociation of CH_4 was highly affected by the Rh cluster size distribution on the surface.

TPR spectra of POX and mixed reforming and results of CH_4–D_2 exchange indicate that CH_4 adsorbs and is activated on Rh/MgO before reaction starts. In fact, all noble metals used in this study were shown to be able to activate CH_4. The activity sequence is Rh > Ru > Pt > Pd (25). The products of the activation are H_{ad} and adsorbed carbon species $(CH_x)_{ad}$ ($x = 0, 1, 2,$ and 3).

In a CH_4 chemisorption experiment, H_2 evolves in advance of the hydrocarbon species. $(CH_x)_{ad}$ ($x = 0, 1, 2,$ and 3)

remains on the surface and is ready to recombine with H or its isotope D to release CH_4 or CH_xD_{4-x} ($x = 0$, 1, 2, and 3) or to react with another atomic or molecular group to form a new molecule. If the new molecule formed is stable, the reactions of $(CH_x)_{ad}$ ($x = 0$, 1, 2, and 3) with other atomic or molecular groups have an advantage in energy and are thermodynamically possible.

CO is very stable in energy with an electronic structure similar to N_2 and it is thermodynamically possible for it to be produced from $(CH_x)_{ad}$ ($x = 0$, 1, 2, and 3). There is no doubt that adsorbed oxygen, O_{ad}, would be the best species to react with $(CH_x)_{ad}$ ($x = 0$, 1, 2, and 3) in syngas production. If sufficient O_{ad} is supplied, syngas will be produced. This is the case in conventional steam reforming and CO_2 reforming or POX. The difference among these processes is the route for supplying O_{ad} and its rate of reaction, namely, the kinetics of reaction.

CO_2 is also very stable in energy and it will be a major by-product in POX. It is likely that gaseous atomic oxygen (O_g) would be responsible for the formation of CO_2 via a homogeneous mechanism and atomic oxygen on the surface (O_{ad}) for the formation of CO via a heterogeneous mechanism (26). The ratio of homogeneous mechanism and heterogeneous mechanism is determined by the concentration of O_g and O_{ad} as well as their kinetics. However, the ratio of CO/CO_2 in the product would have a tendency to reach thermodynamic equilibrium due to the existence of the WGS reaction.

2. In situ Isotope-Labelled $^{13}CO_2$ Transient Experiment for Mixed Reforming

In the *in situ* isotope-labelled $^{13}CO_2$ transient experiment for mixed reforming, most of the ^{13}C is found in the form of ^{13}CO and $^{13}CO_2$. ^{13}CO may come from $^{13}CO_2$ reforming of CH_4. Unlabelled CO_2 may come from the Boudouard reaction and WGS for unlabelled CO. A more important reaction is the oxygen exchange reaction between CO and CO_2, which may be very rapid on the oxide support at high temperature (26).

$$CO + {}^{13}CO_2 \rightleftharpoons {}^{13}CO + CO_2 \qquad [6]$$

Therefore, the amount of ^{13}CO in total CO formation does not represent the rate of $^{13}CO_2$ reforming. However, the amount of labelled carbon ^{13}C in the form of $^{13}CH_4$ is much less than that of ^{13}CO or $^{13}CO_2$.

$^{13}CO_2$ and ^{13}CO adsorbs and decomposes through reactions [7] (27, 28) and [8], respectively.

$$^{13}CO_2 + 2M \rightarrow {}^{13}CO\text{–}M + O\text{–}M \qquad [7]$$

$$^{13}CO + 2M \rightarrow {}^{13}C\text{–}M + O\text{–}M, \qquad [8]$$

where M is the metal. ^{13}C in ^{13}C–M was expected to react with H to form $^{13}CH_4$. As hydrocarbon fragments (CH_x) ($x = 0$, 1, 2, and 3) formed from CH_4 activation are very active on Rh/MgO at experimental conditions, ^{13}C–M formed from ^{13}CO or $^{13}CO_2$ was also expected to be active, and in that case a reasonable amount of $^{13}CH_4$ would be expected in the gas phase. However, the experiment showed a different result. It seems the experimental result supports the explanation that carbon formed from CO or CO_2 is less active than (CH_x) ($x = 0$, 1, 2, and 3) formed from CH_4 activation (8). More kinetics research is required.

3. Mechanism of Mixed Reforming

Decomposition of CO_2 into O_{ad} and CO_{ad} has been discussed in the previous section and decomposition of H_2O in O_{ad} and OH_{ad} has been reported elsewhere (29). As steam reforming and CO_2 reforming start at the same time according to the TPR spectra of mixed reforming, it may suggest that steam reforming and CO_2 reforming share the same type of intermediate. The consumption of the intermediate leads to the formation of CO and the decrease of CO_2 and H_2O. The intermediate is O_{ad} which can be produced from the dissociation of both H_2O and CO_2. The reaction mechanism suggested is that adsorbed carbon species $(CH_x)_{ad}$ ($x = 0$, 1, 2, and 3), formed from activated CH_4, react with adsorbed atomic oxygen O_{ad}, formed from the decomposition of CO_2 and H_2O, and produce CO. The total process of mixed reforming on Rh/MgO is described as follows (M = Rh active site, which is not distinguished for different adsorbing species in the formulas),

(a) $CH_4 + 2M \rightarrow CH_3\text{–}M + H\text{–}M$	
(b) $CH_3\text{–}M + 2M \rightarrow CH\text{–}M + 2\,H\text{–}M$	Activation of CH_4
(c) $CH\text{–}M + M \rightarrow C\text{–}M + H\text{–}M$	
(d) $H_2O + 3M \rightarrow O\text{–}M + 2H\text{–}M$	Decomposition of H_2O
(e) $CO_2 + 2M \rightarrow O\text{–}M + CO\text{–}M$	and CO_2
(f) $CH_x\text{–}M + O\text{–}M + (X-1)M \rightarrow CO\text{–}M + x\,H\text{–}M$	Reaction of adsorbed species
(g) $CO\text{–}M \rightarrow CO + M$	and production of CO and H_2
(h) $2H\text{–}M \rightarrow H_2 + 2M$	

As the main reaction (f) occurs between two adsorbed species, it is a Langmuir–Hinshelwood mechanism. The mechanism is similar to that of steam reforming on Ni catalysts (1) and does not require that CO_2 react by WGS as a first step, giving steam followed by steam reforming as suggested by Bodrov and Apel'baum (10). The reasons are that both steam and CO_2 reforming were found to start simultaneously and no considerable CO_2 decrease and CO increase were observed before reaction starts. As steam reforming and CO_2 reforming have similar reaction mechanisms, their reaction kinetics are expected to be similar, as reported in the literature (1, 10, 15). Moreover, as all noble metals show similar catalytic properties for mixed reforming, it is expected that they will have a similar catalytic mechanism for the reforming reaction. Their activities are determined

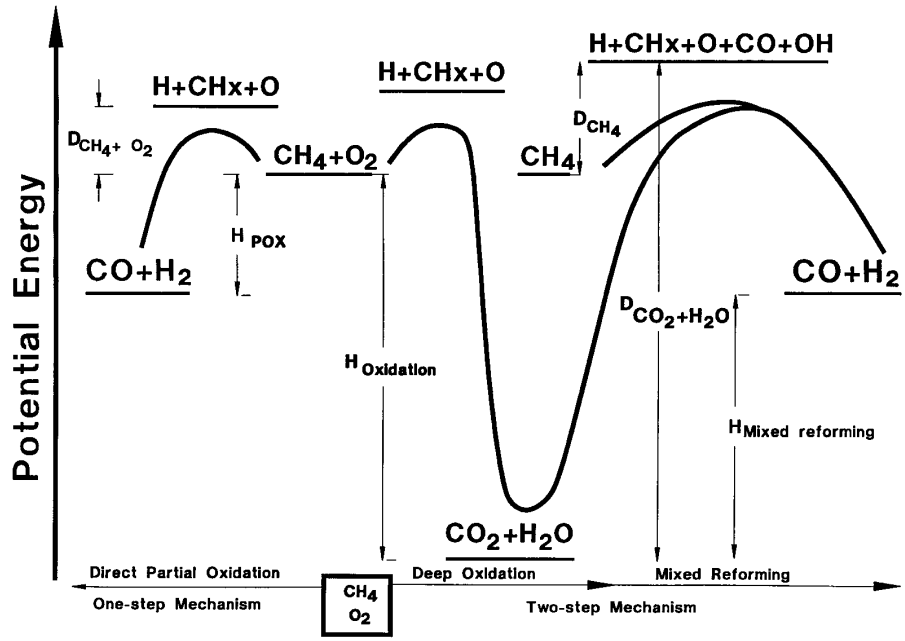

FIG. 9. Scheme for reaction pathways for syngas production from CH_4 and O_2. D, energy of decomposition; H, enthalpy changes of reaction.

by the rate of CH_4 activation and relative stability of the oxygen–metal (O–M) bond for each metal.

4. Mechanism of POX

In mixed reforming, the decomposition of H_2O and CO_2 leads to O_{ad}, which reacts with $(CH_x)_{ad}$ ($x = 0$, 1, 2, and 3) to produce CO. In POX, O_{ad} arises from the decomposition of O_2 and reacts with $(CH_x)_{ad}$ ($x = 0$, 1, 2, and 3) to produce CO.

Due to the high bond energy and stability of an oxygen–metal bond, oxygen chemisorbing on a noble metal is dissociated to atomic oxygen, namely, O_{ad}, above room temperature (26). The O_{ad} is capable of reacting with $(CH_x)_{ad}$ ($x = 0$, 1, 2, and 3) to produce CO. The process can be described as follows.

Activation of CH_4, (a)–(c), is the same as in mixed reforming.

(i) $O_2 + 2M \rightarrow 2O\text{–}M$	Decomposition of O_2
(j) $CH_x\text{–}M + O\text{–}M + (X-1)M \rightarrow CO\text{–}M + x\,H\text{–}M$	Reaction of adsorbed species
(k) $CO\text{–}M \rightarrow CO + M$	and production of CO and H_2
(l) $2H\text{–}M \rightarrow H_2 + 2M$	

This process, the one-step mechanism to produce syngas for POX, is very similar to that of mixed reforming except for using O_2 instead of H_2O and CO_2 to form O–M. The interesting feature is the same type of reactive intermediate, O_{ad}, in the two reactions. It appears that the similarity of the two mechanisms results in the similarity of the two TPR spectra. As there were ignition phenomena for all catalysts and even a noble metal oxide could act as a catalyst and exhibit similar activity as a prereduced metal catalyst, it seems that the O–M consuming reaction (j) is involved in the rate-controlling step of the reaction.

At reaction temperature, O_{ad}, can desorb from the surface and become O_g, which is a stronger and more nonselective oxidant than O_{ad} and, is responsible for deep oxidation of CH_4 to produce CO_2 and H_2O (26). As O_g is very active, it is difficult to avoid deep oxidation under experimental conditions. However, evidence shows that all of the CH_4 does not proceed to syngas via deep oxidation then reforming, the two step mechanism. First, mixed reforming experiments were designed to have the same atomic compositions as POX, equal to 25% CH_4, which in POX was deep oxidised. If POX was via two-step mechanism only, POX and mixed reforming would show similar reactivity. However, experimental results showed that the activity for mixed reforming was much lower than that for POX and H_2/CO ratios exhibited different trends while temperature increased. Second, mixed reforming suffered from strong inhibition from high concentration and coexistence of CO_2 and H_2O, but POX did not. Third, O_2 was not completely consumed in POX, which was expected for a completely deep oxidation. Nevertheless, it is reasonable to suggest that CH_4 partial oxidation to syngas (POX) proceeds by both heterogeneous and homogeneous pathways, because O_{ad} and O_g can coexist at reaction temperature. The amounts of CO and CO_2 as primary products are dependent on the amounts of O_{ad} or O_g and their reaction kinetics. However, the final product distribution is affected by thermodynamic equilibrium. The reaction mechanism for POX is described in Fig. 9.

Because the second step of the two-step mechanism is mixed reforming, which has a high activation energy, and the active sites for CH_4 activation may be inhibited by the high concentration of CO_2 and steam in the reactor, it is unlikely that the preferred reaction mechanism is via the two-step mechanism, at least on the active catalysts Rh/MgO or Ru/MgO. Pd/MgO or Pt/MgO, which have a weak oxygen–metal bond, and in turn a high O_g concentration in the reactor, may have a higher rate for the two-step mechanism; therefore a low CO selectivity was observed for Pd/MgO or Pt/MgO.

5. Effect of the Oxygen–Metal (O–M) Bond Strength

The activation of CH_4 and the reactive ability of intermediate O_{ad} are important steps in the mechanism for POX and mixed reforming and will largely determine the reaction kinetics. Activation of CH_4 is vitally important and is well done by noble metals. The reactive ability of O_{ad} is actually affected by the O–M bond strength or energy. In fact, the involvement of the O–M bond in the reaction kinetics is evident, as pointed out in previous sections.

The O–M bond is involved in two functions for syngas production. First, the formation of O–M assists the decomposition of O_2, H_2O, and CO_2, and second, the decomposition of O–M forms CO with CH_x. For the first function, a high bond strength for O–M is required in order to supply enough energy for the decomposition of O_2, H_2O, and CO_2; for the second function, a weaker bond strength is required in order to allow O–M bond cleavage without a high activation energy. However, a too weak O–M bond might allow oxygen to desorb, thus increasing the selectivity to deep oxidation, as observed on Ag as well as on Pd catalysts (30). The distinctive functions of the O–M bond on the reaction kinetics will lead to a "volcano" curve of activity versus O–M bond strength.

The O–M bond strength can be described quantitatively using the binding energy of oxygen on metals, which is proportional to the heat of adsorption of oxygen or the formation heat of the respective metal oxide (26). The correlation of the CO formation rate with the heat of formation of the most stable oxide for per mole of respective metal (31) is shown in Figs. 10 and 11 for POX and mixed reforming, respectively.

The correlation for POX shows a peak at about 170–270 kJ/mol for each experimental temperature (Fig. 10). Ir, Rh, and Ru are more active than Pt and Pd. Pd and Pt have a relatively weaker O–M bond, which means that they have a strong tendency to release oxygen to O_g and produce more CO_2. From the correlation, it can be expected that a good oxidation catalyst is not equal to a good catalyst for syngas production. Ni is expected to locate at 240 kJ/mol in Fig. 10 for NiO as the stable oxide, near the top position of the curve. However, as easy coking leads to quick deactivation, 0.5% Ni/MgO is not compared in this paper. Nevertheless

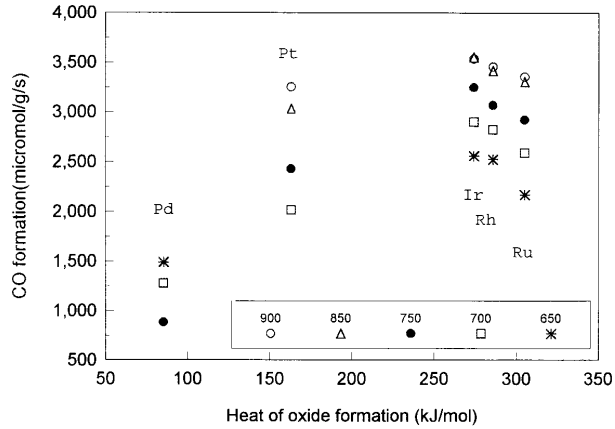

FIG. 10. The correlation of the CO formation rate for POX with the formation heat of the most stable oxide for per mole of the respective metal.

specially treated 7% Ni and 15% Ni samples do show very good activity (30).

The correlation for mixed reforming involved only a half of the volcano curve, as shown in Fig. 11; the other half could not be calculated due to lack of suitable metals. The rate of CO formation increases as the oxide formation heat increases from 80 to 300 kJ/mol at each experimental temperature. Ru, Rh, and Ir have similar oxide formation heat, but Ru and Rh are closer to the top position of the volcano curve. Pt and Pd are less active than Ru, Rh, and Ir as similar to that observed for POX in Fig. 10. The difference of the peak position of the correlation between POX and mixed reforming reflects the fact that the decomposition of CO_2 and H_2O is more difficult than that of O_2, which results in less reaction intermediate O_{ad} produced. A stronger O–M bond is required in order to obtain more O_{ad}, and therefore the peak position is shifted to a higher energy for mixed reforming. It appears that temperature has little effect on the

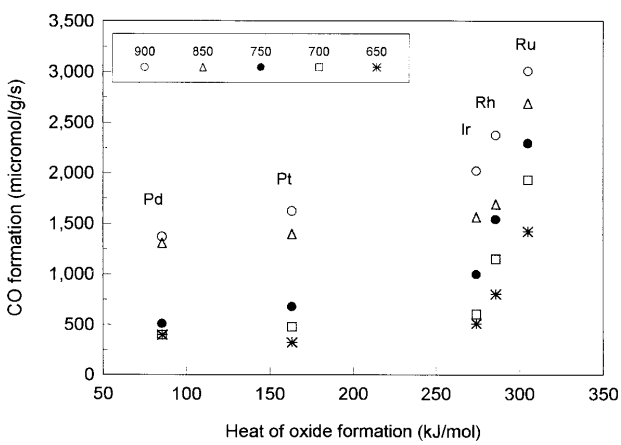

FIG. 11. The correlation of the CO formation rate for mixed reforming with the formation heat of the most stable oxide for per mole of the respective metal.

peak position of the curve for POX and mixed reforming under the selected experimental conditions.

It has been pointed out that the rate of CO formation is controlled by two factors, the rate of CH_4 activation and the O–M bond strength. In most cases, catalysts are bifunctional but quantitative analysis of each function needs further investigation.

CONCLUSION

By using temperature-programmed reaction, isotope transient techniques, and reactivity evaluation for partial oxidation (POX) and mixed reforming of CH_4 at high-space velocity of $5.5 \times 10^5\ h^{-1}$, it is found that:

1. In mixed reforming, CO_2 reforming and steam reforming start simultaneously, which implies that both reformings have a similar type of reaction intermediate. The mechanism of mixed reforming is suggested. Mixed reforming showed a changing H_2/CO ratio with increased temperature;

2. POX has a similar type of reaction intermediate O_{ad} to mixed reforming despite the fact that POX showed much higher activity than mixed reforming, although their C, H, and O atomic concentrations were the same at the beginning of each reaction. It is suggested that the lower rate of reaction in mixed reforming is due to the blocking of active sites for CH_4 activation by CO_2 and H_2O;

3. POX proceeds via both one-step and two-step mechanisms; the ratio for each mechanism is dependent on the concentration and kinetics of adsorbed atomic oxygen and gaseous atomic oxygen;

4. Rh/MgO without previous reduction treatment also showed a high reactivity for POX but with a higher ignition temperature than a prereduced catalyst.

5. Correlation of CO formation rate for POX and mixed reforming with oxide formation heat shows a volcano-shaped curve. The peak of the curve for POX locates at 170–270 kJ/mol, that for mixed reforming locates at a value higher than 300 kJ/mol;

6. An *in situ* isotope-labelled $^{13}CO_2$ transient experiment for mixed reforming indicated that carbon formed from CO_2 or CO decomposition was less active than $(CH_x)_{ad}$ ($x = 0$, 1, 2, and 3) formed from CH_4 decomposition.

7. For POX, a small amount of steam has little effect on the CO formation rate for an active catalyst but decreases the rate for a less active catalyst.

ACKNOWLEDGMENT

Daiyi Qin acknowledges the postdoctoral research fellowship provided by CSIRO. The authors also thank Mr. I. Campbell and Mrs. J. Chipperfield for their help and assistance with the experiments and this manuscript.

REFERENCES

1. Rostrup-Nielsen, J. R., *in* "Catalysis, Science and Technology" (J. R. Anderson and M. Boudart, Eds.), Vol. 5, Chap. 1. Springer-Verlag, Berlin, New York, 1984.
2. Ashcroft, A. T., Vernon, P. D. F., and Green, M. L. H., *Nature* **344**, 319 (1990).
3. Vermeiren, W. J. M., Blomsma, E., and Jacobs, P. A., *Catal. Today* **13**, 427 (1992).
4. Dissanayake, D., Rosynek, M. P., Kharas, K. C., and Lunsford, J. H., *J. Catal.* **132**, 117 (1991).
5. Hickman, D. A., Haupfear, E. A., and Schmidt, L. D., *Catal. Lett.* **17**, 223 (1993); Hickman, D. A., and Schmidt, L. D., *J. Catal.* **138**, 267 (1992); Hickman, D. A., and Schmidt, L. D., *Science* **259**, 343 (1993).
6. Choudhary, V. R., Rajput, A. M., and Rane, V. H., *Catal. Lett.* **16**, 269 (1992); Choudhary, V. R., Rajput, A. M., and Prabhakar, B., *Catal. Lett.* **15**, 363 (1992); Choudhary, V. R., Sansare, S. D., and Mamman, A. S., *Appl. Catal.* **A90**, L1–L5 (1992).
7. Lapszewicz, J., and Jiang, X-Z., *in* "Symposium on Natural Gas Upgrading II, Division of Petroleum Chemistry, Inc. & American Chemical Society, San Francisco April 5–10, 1992," p. 252.
8. Rostrup-Nielsen, J. R., and Bak Hansen, J-H., *J. Catal.* **144**, 38 (1993).
9. Fish, J. D., and Hawn, D. C., *Solar Energy Eng.* **109**, 215 (1987); Gadalla, A. M., and Sommer, M. E., *Chem. Eng. Sci.* **44**(12), 2825 (1989).
10. Bodrov, I. M., and Apel'baum, L. O., *Kinet Katal.* **8**, 379 (1967).
11. Richardson, J. T., and Paripatyadar, S. A., *Appl. Catal.* **61**, 293 (1990).
12. Udengaad, N. R., Bak Hansen, J-H, Hansen, D. C., and Stal, J. A., *Oil Gas J.* **90**, 62 (1992).
13. Topfer, H. J., *Gas Wasserfach* **117**, 412 (1976).
14. Tenner, S., *Hydrocarbon Process* **66**, 52 (1987).
15. Rostrup-Nielsen, J. R., Christiansen, L. J., and Bak Hansen, J-H, *Appl. Catal.* **43**, 287 (1988).
16. Erdöhelyi, A., Cserenyi, J., and Solymosi, F., *J. Catal.* **141**, 287 (1993).
17. Lapszewicz, J., and Jiang, X-Z., *in* "Symposium on Chemistry and Characterisation of Supported Metal Catalysts, American Chemical Society, Chicago, IL, Aug. 22–27, 1993."
18. Dissanayake, D., Rosynek, M. P., and Lunsford, J. H., *J. Phys. Chem.* **97**, 3644 (1993).
19. Chang, Y-F., and Heinemann, H., *Catal. Lett.* **21**, 215 (1993).
20. Ross, J. R. H., Steel, M. C. F., and Zeini-Isfahani, A., *in* "Mechanisms of Hydrocarbon Reactions" (F. Marta and D. Kallo, Eds.), Budapest, 1975.
21. Qin, D., and Lapszewicz, J., *Catal. Today* **21**, 551 (1994).
22. Lobo, L. S., Trimm, D. L., and Figueiredo, *in* "Proceedings, 5th International Congress on Catalysis, Palm Beach, 1972" (J. W. Hightower, Ed.), Vol. 2, p. 1125. North Holland, Amsterdam, 1973.
23. Kemball, C., *Catal. Rev.* **5**(1), 33 (1971).
24. Frennet, A., Lienard, G., Crucq, A., and Degols, L., *J. Catal.* **53**, 150 (1978).
25. Lapszewicz, J., Ekstrom, A., Qin, D., and Jiang, X., *in* "International Conference on Catalysis and Catalytic Processing, Cape Town, South Africa, Oct. 24–27, 1993."
26. Boreskov, G. K., *in* "Catalysis, Science and Technology" (J. R. Anderson and M. Boudart, Eds.), Vol. 3, Chap. 2. Springer-Verlag, Berlin/New York, 1982.
27. Solymosi, F., and Pasztor, M., *J. Catal.* **104**, 312 (1987).
28. Solymosi, F., *J. Mol. Catal.* **65**, 337 (1991).
29. Heras, J. M., and Viscido, L., *Catal. Rev. Sci. Eng.* **30**, 281 (1988).
30. Qin, D., Lapszewicz, J., and Ekstrom, A., unpublished data.
31. "Lange's Handbook of Chemistry (13th)" (J. A. Dean, Ed.), McGraw–Hill, New York, 1985.